MTL TR 87-52

AD

AD-A186 989

WIRE-CUT ELECTRICAL DISCHARGE MACHINABILITY OF CERAMICS

WILLIAM S. RICCI, HOLLY A. SKEELE, and WILLIAM R. BLUMENTHAL

PROCESSING TECHNOLOGY DIVISION

September 1987

US ARMY
LABORATORY COMMAND
MATERIALS TECHNOLOGY
LABORATORY

U.S. ARMY MATERIALS TECHNOLOGY LABORATORY
Watertown, Massachusetts 02172-0001

REPORT DOCUMENTATION PAGE

READ INSTRUCTIONS BEFORE COMPLETING FORM

1. REPORT NUMBER: MTL TR 87-52
2. GOVT ACCESSION NO:
3. RECIPIENT'S CATALOG NUMBER:

4. TITLE (and Subtitle): WIRE-CUT ELECTRICAL DISCHARGE MACHINABILITY OF CERAMICS
5. TYPE OF REPORT & PERIOD COVERED: Final Report
6. PERFORMING ORG. REPORT NUMBER:

7. AUTHOR(s): William S. Ricci, Holly A. Skeele, and William R. Blumenthal
8. CONTRACT OR GRANT NUMBER(s):

9. PERFORMING ORGANIZATION NAME AND ADDRESS: U.S. Army Materials Technology Laboratory, Watertown, Massachusetts 02172-0001, SLCMT-MCD
10. PROGRAM ELEMENT, PROJECT, TASK AREA & WORK UNIT NUMBERS: D/A Project: 1L263102D071, Agency Accession: DA 30 3398

11. CONTROLLING OFFICE NAME AND ADDRESS: U.S. Army Laboratory Command, 2800 Powder Mill Road, Adelphi, Maryland 20783-1145
12. REPORT DATE: September 1987
13. NUMBER OF PAGES: 23

14. MONITORING AGENCY NAME & ADDRESS (if different from Controlling Office):
15. SECURITY CLASS. (of this report): Unclassified
15a. DECLASSIFICATION/DOWNGRADING SCHEDULE:

16. DISTRIBUTION STATEMENT (of this Report):

Accession For	
NTIS GRA&I	☑
DTIC TAB	☐
Unannounced	☐
Justification	
By	
Distribution/	
Availability Codes	
Dist	Avail and/or Special
A-1	

17. DISTRIBUTION STATEMENT (of the abstract entered in Block 20, if different from Report):

18. SUPPLEMENTARY NOTES:

INSPECTED 4

19. KEY WORDS (Continue on reverse side if necessary and identify by block number)

Ceramics	Machining	Silicon carbide
Diamond grind	Residual stress	Boron carbide
Electrical discharge	Titanium diboride	Fracture strength

20. ABSTRACT (Continue on reverse side if necessary and identify by block number)

(SEE REVERSE SIDE)

Block No. 20

ABSTRACT

The wire-cut electrical discharge machinability of four ceramics was evaluated. Titanium diboride and silicon carbide workpieces were successfully cut in the monolithic state. Boron carbide could only be cut when a metallic sandwich structure was placed around the workpiece. Silicon nitride could not be successfully cut. Mechanisms of material removal as well as a minimum level of workpiece electrical conductance necessary for EDM are proposed.

Characterization of the surface damage resulting from electrical discharge machining is presented. Recast, partially melted, and heat affected zones are identified. The effects of parametric processing variations on surface integrity are discussed. Flexure strength and residual stress data are compared for EDM cut and diamond ground surfaces in titanium diboride. Certain limitations are proposed for the EDM fabrication of ceramic components where surface defects are strength limiting.

CONTENTS

INTRODUCTION

Electrical discharge machining (EDM) has been used for the complex shaping of metal components to very high tolerance for many years. However, electrical discharge machining has not been used extensively for ceramics. The application of traditional machining methods to finished ceramics is difficult or impossible due to the lack of ductility and the superior thermomechanical properties of ceramics. Diamond abrasive machining is necessarily and extensively used in the ceramics industry, but there are many limitations to its use. Foremost is the restricted shapes that can be produced. Further, highly skilled labor is necessary due to precise setup and operating conditions, which are not readily amenable to automation. Equipment and tooling costs are also high, and machine tool wear is rapid due to the high workpiece hardness and the extreme stresses generated during machining.

Unlike abrasive machining, the wire EDM tool does not contact the workpiece and does not exert a direct mechanical force on it. Such contact stresses are integral to diamond machining, and, if not uniformly controlled, can produce severe subsurface cracking resulting in an increased susceptibility of machined surfaces to brittle failure.[1] The mechanisms of material removal and the nature or condition of the resultant surfaces created on the strength and fracture properties of abrasive machined ceramics have previously been studied.[2-4]

The mechanism of material removal in wire-cut electrical discharge machining involves the complex erosion effect from electric arcs generated by a pulsating direct current power supply. The arcs occur between two closely spaced electrodes in the presence of deionized water. The cathode is an expendable, continuously fed wire that advances into the anode, which is the stationary workpiece. A conclusive theory has not been established for this complex process; however, empirical evidence suggests the following events take place. First, as the electrodes are brought in close proximity, a powerful electric current rapidly (in 10^{-7} to 10^{-8} sec) vaporizes a small amount of both electrodes to form localized plasma channels of very high conductivity. The actual discharge then takes place with a heavy flow of current that concurrently generates a powerful magnetic field. This magnetic field compresses the current beam cross section and results in localized heating up to 10,000°C. This high energy density causes local melting and vaporization of a portion of the wire and the workpiece, which is the dominant erosion process. During the cyclic discharge and heating periods, material can be ejected violently, as evidenced by the formation of surface craters primarily on the anode (workpiece). Some collateral mechanical erosion also occurs due to debris impacts. Melted surface layers that are not completely removed resolidify as a recast layer. The character of the resultant surface depends upon the discharge energy, which is a function of equipment parameters such as current, gap voltage, and pulse duration. There remains, however, a question as to whether the high temperature gradients inherent in the EDM process also induce subsurface thermal residual stresses and cracks that could significantly degrade mechanical properties especially in ceramics with traditionally low thermal conductivities.

1. STOKES, R.J. *Effects of Surface Finishing on Mechanical and Other Physical Properties of Ceramics.* The Science of Ceramic Machining and Surface Finishing, NBS Special Publication 348, May 1972, p. 343-351.
2. HAWMAN, M.W., COHEN, P.H., CONWAY, J.C., and PANGBORN, R.N. *The Effect of Grinding on the Flexural Strength of Sialon Ceramic.* J. Mat. Sci., v. 20, 1985, p. 482-490.
3. RICE, R.W., and MECHOLSKY, J.J. *The Nature of Strength Controlling Machining Flaws in Ceramics.* Naval Research Laboratory Memorandum Report 4077, September 25, 1979, (ADA075481).
4. RICE, R.W. *Machining of Ceramics.* Proc. of the Second Army Materials Technology Conference on Ceramics for High Performance Applications, Army Materials and Mechanics Research Center, Watertown, Massachusetts, November 13-16, 1983.

Our evidence suggests that wire-cut EDM could be a viable alternative for the shaping of complex ceramic contours that have not been possible with conventional diamond machining. In particular, the EDM process is essentially independent of workpiece ductility and hardness; very thick parts can be multi-axially shaped; tool wear is not a major concern; and the operation can be completely automated. A review of the operation of the wire EDM process has been presented elsewhere.[5]

The primary reasons for the limited growth in the utilization of the EDM process for ceramic machining include low material removal rates[6] and the fact that the process is, by and large, limited to materials with reasonably good electrical conductivities[7] (e.g., metals and intermetallic compounds of certain carbides, borides, nitrides and silicides). A minimum workpiece conductance value for the EDM process has not, however, been established from prior investigations.

Recently, the increased use of non-oxide ceramics with adequate electrical conductivity has stimulated interest in the use of EDM for ceramics. Some investigators[8-10] have attempted to improve the electrical discharge machinability of ceramics, particularly silicon nitride and silicon carbide, by increasing the bulk electrical conductivity through minor additions of borides, carbides and nitrides. Although the results of this work are encouraging, the corresponding effects of these additions on the mechanical properties of the bulk material and on EDM cut surfaces have not been fully evaluated.

In this report, the wire-cut electrical discharge machinability of four ceramics (titanium diboride, silicon carbide, boron carbide, and silicon nitride) will be discussed. To improve the electrical discharge machinability of those ceramics that cannot ordinarily be wire EDM cut in the monolithic state, setups using metallic sandwich structures formed about the workpiece were evaluated. This was done in an attempt to induce spark generation and thereby initiate cutting.

The effects of wire-cut electrical discharge machining on the surface condition and subsequent fracture properties of the aforementioned ceramic materials were also evaluated. A comparison between wire EDM and diamond grinding will be discussed in this report.

EXPERIMENTAL

Electrical discharge machinability tests were performed using an Elox Series P wire-cut EDM system with a DU 3008 power supply. Flushing nozzles were located 0.02-0.03" above and below the workpiece, and a 0.010" diameter brass wire was used in all experiments. Specific cutting parameters for the materials with their respective thicknesses are presented later in this report for both roughing cuts and finishing passes.

5. *Machining Data Handbook.* 3rd Ed., v. 2, Metcut Research Associates, Cincinnati, Ohio, 1980, p. 12-49.
6. MACCALOUS, J.W., and COPPFER, W.P. *Electrical Discharge Machining of Zirconium Diboride.* Proc. AIAA/ASME/SAE 13th Structures, Structural Dynamics and Materials Conference, San Antonio, Texas, April 10-12, 1972, v. 2, Materials, Paper No. 72-329.
7. LEE, D.W., and FEICK, G. *The Techniques and Mechanisms of Chemical, Electrochemical and Electrical Discharge Machining of Ceramic Materials.* The Science of Ceramic Machining and Surface Finishing, Proc. of Symposium at NBS, Gaithersburg, Maryland, November 2-4, 1970, National Bureau of Standards, p. 197-211.
8. KAMIJO, E., HONDA, M., HIGUCHI, M., TAKEUCHI, H., and TANIMURA, T. *Electrical Discharge Machinable Si_3N_4 Ceramics.* Sumitomo Electric Technical Review, no. 24, January 1985, p. 183-190.
9. JANNEY, M.A. *Mechanical Properties and Oxidation Behavior of a Hot-Pressed SiC-15 Vol% TiB_2 Composite.* Amer. Cer. Soc. Bull., v. 66, 1987, p. 322-324.
10. McMURTRY, C.H., BOECKER, W.D.G., SESHADRI, S.G., ZANGHI, J.S., and GARNIER, J.E. *Microstructure and Material Properties of SiC-TiB_2 Particulate Composites.* Amer. Cer. Soc. Bull., v. 66, 1987, p. 325-329.

Silicon carbide (SiC), silicon nitride (Si_3N_4), boron carbide (B_4C), and two grades of titanium diboride (TiB_2) workpieces were evaluated. Electrical conductivities of the ceramics were measured, and are listed in Table 1. It should be noted that the B_4C was near stoichiometric, Grade A TiB_2 was 99% pure, Grade B TiB_2 was ~95% pure, and the SiC was siliconized. The addition of free Si to the SiC ceramic resulted in a dramatic increase in electrical conductivity over that of purer material.

Table 1. ROOM TEMPERATURE ELECTRICAL CONDUCTIVITY VALUES FOR WORKPIECES TESTED

Workpiece	Electrical Conductivity $(ohm\text{-}cm)^{-1}$
TiB_2	6.9×10^{4}*
SiC	2.9×10^{-2}
B_4C	1.6×10^{-2}
Si_3N_4	5.0×10^{-14}*

*Reference 11

Cross sections of cut edges were prepared for SEM evaluation of Grade B TiB_2 by slicing and polishing, followed by etching with a $2HF:1HNO_3$:1 glycol solution. As-machined surfaces and fracture surfaces across EDM cut edges were also evaluated by SEM. Fracture surfaces were prepared by first slicing parallel to an EDM cut edge and then fracturing the resultant thin plate by four-point bending. Each EDM cut surface to be fractured was placed in the bend jig so it would initially be in compression.

Thirty MIL-STD 1942 (MR) size B flexural specimens were wire electrical discharge machined from a bulk piece of hot pressed Grade A TiB_2. A like number were diamond ground from the same billet of material. Both groups of specimens were loaded to failure in four-point bending in accordance with MIL-STD 1942 (MR). Fracture surfaces were examined to determine flaw origins.

Fractured EDM specimens exhibiting equivalent strengths were further evaluated by X-ray diffraction and SEM microprobe techniques for the existence of residual stresses or chemical reactions near the surfaces. As-cut EDM machined surfaces, mechanically polished EDM surfaces, and diamond ground surfaces were examined. The three polished EDM samples were polished to remove 70, 100, and 130 micron thick layers from the surface.

Residual stresses were measured using the diffractometer technique,[12] with CuKα radiation diffracted from the (212) crystallographic planes at about 131.5° 2θ. The incident beam was angled at 12 and 22 degrees to the sample surface normal to provide two ψ angles at each inclination of about ±12 and 36, and ±2 and 46 degrees, respectively. A Young's modulus of 549×10^3 MPa and Poisson's ratio of

11. SAMSONOV, G.V. *Plenum Press Handbook of High-Temperature Materials, Properties Index*. Plenum Press, New York, 1964, p. 142-147.
12. *SAE Residual Stress Measurement by X-Ray Diffraction, SAE J784a*. Soc. of Auto. Eng. Inc., Warrendale, PA, 1971.

0.105 were used for analytic calculations of stresses. It should be noted that these elastic constants are bulk values and not necessarily the absolute value for the (212) plane in a stressed polycrystalline sample.[13] Empirical values for E and ν developed specifically for X-ray diffraction stress measurements are preferred,[14] but a calibration sample suitable for X-ray experiments to provide these values was not available. Both the single exposure and $\sin^2 \psi$ techniques[15] were used to determine the residual stresses.

Surface finish on the diamond ground and EDM cut surfaces was measured with a micrometrical profilometer, type QB, and R_a values were reported.

RESULTS

Wire electrical discharge machining parameters and resultant material removal rates for the TiB_2, SiC, and B_4C workpieces are shown in Table 2. The B_4C sample could not be cut in the monolithic state, but it was successfully cut when a single 1/8" thick sheet of brass was placed on its top surface. The Si_3N_4 workpiece could not be cut in either the monolithic state or when 1/4" thick copper plates were placed on both the top and bottom surfaces. Resultant surface finish values of successful cuts are included in Table 2.

Table 2. WIRE-CUT ELECTRICAL DISCHARGE MACHINING PARAMETERS

Sample Number	Workpiece Material	Thickness (in.)	On Time (μsec)	Off Time (μsec)	Offset (in.)	Gap Voltage (V)	Gap Current (A)	Servo Voltage (V)	No Load Voltage (V)	Wire Feed (ipm)	Wire Tension (gr)	Indicated Feed Rate (ipm)	Material Removal Rate** (in.²/hr)	Surface Roughness (μin. R_a)
1	TiB_2	0.5	7	7	-	45	6	16	7	10	900	0.200	6.0	60
	TiB_2													
2a	Roughing Cut	3.5	8	12	-	N/R*	9	17	8	10	1100	0.662	1.3	70
2b	1st Finishing	3.5	3	8	0.003	N/R	1	17	11	8	1100	0.712		55
2c	2nd Finishing	3.5	1	8	0.0005	N/R	0.7	17	13	8	1100	0.400		45
2d	3rd Finishing	3.5	1	8	0	45	0.5	17	10	8	1100	0.025		30
3	SiC	0.6	7	12	-	65	3	18	9	10	900	0.225	2.4	60
	SiC													
4a	Roughing Cut	1.0	6	40	-	N/R	N/R	17	8	10	1100	N/R		70
4b	1st Finishing	1.0	2	10	0.001	150	1	20	15	10	1100	0.365		55
4c	2nd Finishing	1.0	1	6	0.0005	120	0.6	17	13	10	1100	N/R		50
4d	3rd Finishing	1.0	1	6	0	N/R	N/R	17	13	10	1100	N/R		45
5	B_4C	0.4	5	35	-	*	2	25	12	10	1100	0.020	0.5	95
6	Si_3N_4	0.3	Could Not Cut Even With Metallic Sandwich Configuration											

*Not recorded

**Material removal rate = feed rate X thickness X 60

Thermal responses of the Grade B TiB_2 workpiece microstructure to EDM include a recast layer at the cut surface, a subsurface zone with grain boundary melting, and a heat affected zone. Recast layers, in which the material was fully melted and

13. RUUD, C.O. *X-Ray Analysis and Advances in Portable Field Instrumentation.* J. Metals, v. 31, no. 6, July 1979, p. 10-15.
14. RUUD, C.O., SNOHA, D.J., and IVKOVICH, D.P. *Experimental Methods for Determination of Precision and Estimation of Accuracy in XRD Residual Stress Measurement.* Adv. in X-Ray Anal., v. 30, 1987.
15. DOLLE, H. *The Influence of Multiaxial Stress State, Stress Gradients and Elastic Anisotropy on the Evaluation of Residual Stress by X-Rays.* J. Appl. Cryst., v. 12, 1979, p. 489-510.

resolidified, were ~2.5-8.0 μm thick, and could be seen in both polished and fractured surfaces (Figures 1 and 2) for TiB_2. A more dramatic view of a recast surface layer is shown in Figure 3 for a wire cut in the SiC workpiece that passed through a large grain.

Partially melted zones, in which the grain boundaries appear to have been liquefied, were within one to two grain diameters from the cut surface. This zone is most easily discerned by the smooth, rounded grains and overetched grain boundaries (Figure 1).

The heat affected zone, distinguished by a 50 μm wide region of grain boundary directionality planar to the cut surface, was also seen in the polished and etched sample of Grade B TiB_2 shown in Figure 1. Grain boundary directionality was confirmed by examination of a corner cut (Figure 4) for which grains near the cut edge are oriented parallel to the contour of the cut surface. As a further confirmation of the presence of a heat affected zone, SEM examination of a fracture surface through a cut edge (Figure 5) revealed higher concentrations of porosity and almost 100% intergranular fracture within 50 μm of the cut edge compared with ~50% intergranular fracture in the bulk material.

Also occurring within the heat affected zone is a significant degree of grain refinement (~50%, Figure 1). There may have been some grain growth behind this region, but this was not readily discernible in either the polished or fracture surface specimens. The effects of material purity and possibly grain size are evident by comparing the fracture surfaces of grade B TiB_2 (Figures 1, 4, and 5) and the purer grade A TiB_2 (Figures 2 and 6). The presence of a low melting grain boundary phase can, therefore, significantly increase microstructural changes during EDM cutting.

Comparison between Figures 2 and 6 shows the effect of heat input on surface quality and depth of the recast layer for cuts in grade A TiB_2. Recast layer depth for the higher heat input roughing cut was ~7.5 μm (Figure 6) compared to 3 μm for the low heat input skim cut (Figure 2). Variations in surface roughness and integrity for the two TiB_2 cutting conditions can be seen at both low angles (Figures 2 and 6) and high angles (Figures 7 and 8) with respect to the cut surface. The higher heat input surface (Figure 8) had a heavier and coarser distribution of slag and a higher concentration of porosity and microcracks. Similar results are shown for SiC in Figure 9. SEM examination of fractured surfaces of all cut samples showed that microcracks existing in the slag/recast layer do not extend into the base material. Even though increased heat input is expected to increase heat affected zone size, no discernible differences could be derived from the appearance of fracture surfaces.

Variations in workpiece microstructure and porosity were shown to affect thermal changes and machinability. In SiC with a mixed grain size microstructure, fine grains were always preferentially removed or melted at the cutting interface (Figure 10). In B_4C, areas with high levels of porosity also showed the same tendency for preferential removal (Figure 11).

It was stated earlier that the B_4C workpiece could only be cut when a strip of brass was attached to its top surfaces. Figure 12 illustrates the as-cut surface, showing the same surface melting features as those of SiC and TiB_2. EDAX spectroscopy also did not reveal any Cu or Zn residues on the surface, indicating that swarf from the sandwich plate was not largely redeposited in the cut area.

Flexure test results for both wire-cut EDM and diamond ground grade A TiB_2 specimens are shown in Table 3. Characteristic strength values of the bend specimens for the electrical discharge machined specimens were 23% lower than those of specimens diamond machined. The Weibull moduli for both tests were high (>24), and examination of fracture surfaces indicated that strength limiting flaws originated over 90% of the time from the surface.

Table 3. FLEXURE TEST RESULTS FOR TiB_2 SPECIMENS DIAMOND GROUND AND WIRE CUT ELECTRICAL DISCHARGE MACHINED

	Strength (MPa)	Modulus (90% Confidence)
Diamond Ground	398	28.7 ± 0.6
Wire-Cut EDM	305	24.4 ± 0.5

The residual stresses for the diamond ground surfaces were generally compressive. One sample showed values ranging from 0 to -261 MPa. The other sample generally showed compressive stresses of about -268 MPa, but, in one region, tensile stresses of about 577 MPa were indicated.

The two EDM as-cut surfaces showed stress gradients with depth that were tensile. One sample showed a tensile stress of about 275 MPa at the surface to slightly compressive at depths of 10-15 μm. The other showed a similar gradient with surface stresses at 352 MPa and a compressive stress of about -310 MPa at depths of 10-20 μm.

The EDM sample with 70 μm of surface removed showed a compressive stress of -437 MPa. The sample with 100 μm removed showed compressive stress of -303 MPa. The sample with 130 μm removed showed a surface compressive stress gradient from 0 to -331 MPa.

X-ray diffraction and SEM microprobe analysis failed to reveal chemical changes to the surface such as segregation of impurities, phase changes, or contamination. However, the detection level of these analyses is not adequate to observe significant changes in grain boundary chemistry.

DISCUSSION

The minimum electrical conductivity of ceramic materials required for electrical discharge machining appears to be in the range of 2×10^{-2} $(ohm\text{-}cm)^{-1}$. This was shown by the ability to induce spark generation and to initiate the cutting of the B_4C/brass sandwich. The reason for the success in cutting the B_4C is not exactly known, but it could be a result of the local increase in electrical conductivity, due to increased electron mobility or the formation/elimination of new surface phases such as boron oxide, at the higher temperatures present during machining.

Material removal rates for the ceramics tested in this exploratory work were relatively low, but the corresponding surface finishes produced were reasonably good. For complex contours, wire EDM cutting speeds are considered to be superior

to those of any abrasive grinding process. Improvements in machining performance may be expected for other ceramics containing low melting or higher conductivity grain boundary constituents and by tailoring ceramic microstructures.

Properly performed diamond grinding results in a 5-25 μm deep damage zone with a high concentration of microcracks on machined ceramic surfaces.* The altered surface zone for wire EDM was found to be ~20-50 μm deep. In the limited work performed, any high induced thermal gradients and their resultant tensile residual stresses were not found to generate large macrocracks at the EDM machined surface. However, the 50 μm altered zone from EDM with many potential defect sites will have a negative affect on strength and fracture toughness properties, especially for thin, surface flaw sensitive ceramic components (i.e., turbine blades).

The combination of large surface tensile stresses and sub-surface compressive stresses could support stable surface flaw networks contributing to the reduced fracture strength observed for wire-cut EDM samples. Another contributing factor to the observed lowering of fracture strength is surface roughness. A typical roughness value for an EDM surface is 2 μm R_a, and 0.30 μm R_a for diamond ground surfaces. Two microns is only the average roughness. The extreme values in roughness for EDM surfaces may reach 20 μm, the depth of several grains. Note that the wire orientation during cutting was parallel to the axis of the flexure bars, thereby minimizing variations in cutting depth due to wire movement.

A third factor is the large amount of porosity that can be found in the recast layer and on the surface (Figure 13). These individual pores will interact and tend to behave like a much larger pore in addition to lowering the local fracture toughness of the material.

Finally, chemical alterations to the surface such as contamination from the wire electrode, segregation and diffusion of impurities at the grain boundaries, and the creation of new phases or compounds due to the high temperature conditions, will lower the surface fracture toughness without requiring the presence of subsurface cracking as the origin of failure.

Possible methods for countering the negative EDM surface effect on strength for critical components include: (1) finish machining by abrasive means, with a depth cut not to exceed 2.5 μm per pass, to reduce surface roughness and remove the thermally/chemically altered zone, and (2) thermally annealing the workpiece to relieve residual stresses and heal possible subsurface and surface cracking.

CONCLUSIONS

Titanium diboride and silicon carbide workpieces were successfully cut by the wire EDM process. Boron carbide workpieces could not be cut in the monolithic state; however, when a 1/8" thick brass strip was placed on the top surfaces, cutting was possible. Silicon nitride could not be cut in either the monolithic state or when a 1/4" copper sandwich structure was placed about the workpiece in an attempt to induce spark generation and initiate cutting.

Success in cutting the boron carbide is believed to be due to the effects of the local increase in electrical conductivity, due to increased electron mobility

*QUINN, G.D. U.S. Army Materials Technology Laboratory, Watertown, Massachusetts, private communication, July 1986.

and possibly the formation of new surface phases, at the higher temperatures present during machining.

The ability to cut boron carbide with a conductive cover plate sandwich indicates that the minimum level of electrical conductance required for the electrical discharge machining of ceramics appears to be in the range of 2×10^{-2} $(ohm\text{-}cm)^{-1}$. Since it was found that fine grains were preferentially removed during EDM, it may be expected that further improvements with other fine grain ceramics and those containing low melting or higher conductivity grain boundary constituents will also make these materials more amenable to EDM.

Electrical discharge machining resulted in, at most, a 50 μm thermally affected surface on ceramic workpieces. This surface zone consisted of a recast layer followed by partially melted and heat affected zones. The recast layer was typically 3-8 μm deep. The partially melted grain boundary zone extended one to two grain diameters from the surface, and was characterized by grain boundaries that appeared to have been liquefied. The heat affected zone was characterized by a significant degree of grain refinement (~50%), and possibly some grain growth and higher concentrations of porosity. In addition, fracture surfaces through EDM cut surfaces revealed lower levels of transgranular fracture within the heat affected zone, indicating other microstructural changes.

Parametric variations, mainly heat input, required for roughing and skim cuts resulted in corresponding changes in the thermally affected zone. Recast layer thickness for skim cuts was less than half that of roughing cuts. Heavier and coarser slag distributions as well as higher concentrations of porosity and microcracks in the slag were also noted on rough cut surfaces. Microcracks were not, however, observed to extend into the heat affected zone or unaffected base material.

Residual stress values were determined at and beneath the EDM cut surface for TiB_2. Residual stresses at the EDM surface were largely tensile in nature. Residual stresses at the surface of diamond ground and polished EDM specimens were compressive.

Flexure tests with TiB_2 comparing wire-cut EDM with diamond ground samples showed that EDM samples have a 23% reduction in strength over diamond ground ones. The reasons for this decrease are not conclusive, but are thought to be due to a combination of surface roughness and tensile stresses as well as the lowering of the surface fracture toughness due to porosity and chemical alteration.

Even though material removal rates were low for the ceramics tested, wire EDM should be considered a viable alternative for the shaping of complex ceramic contours, since this is extremely difficult if not impossible by standard abrasive grinding methods. However, it is believed that the electrical discharge machining of small surface critical components will require secondary finish machining or annealing operations to assure removal of any deleterious effects on fracture strength and toughness properties.

ACKNOWLEDGEMENT

The authors wish to thank Dr. Clayton Ruud of The Pennsylvania State University for providing the residual stress data.

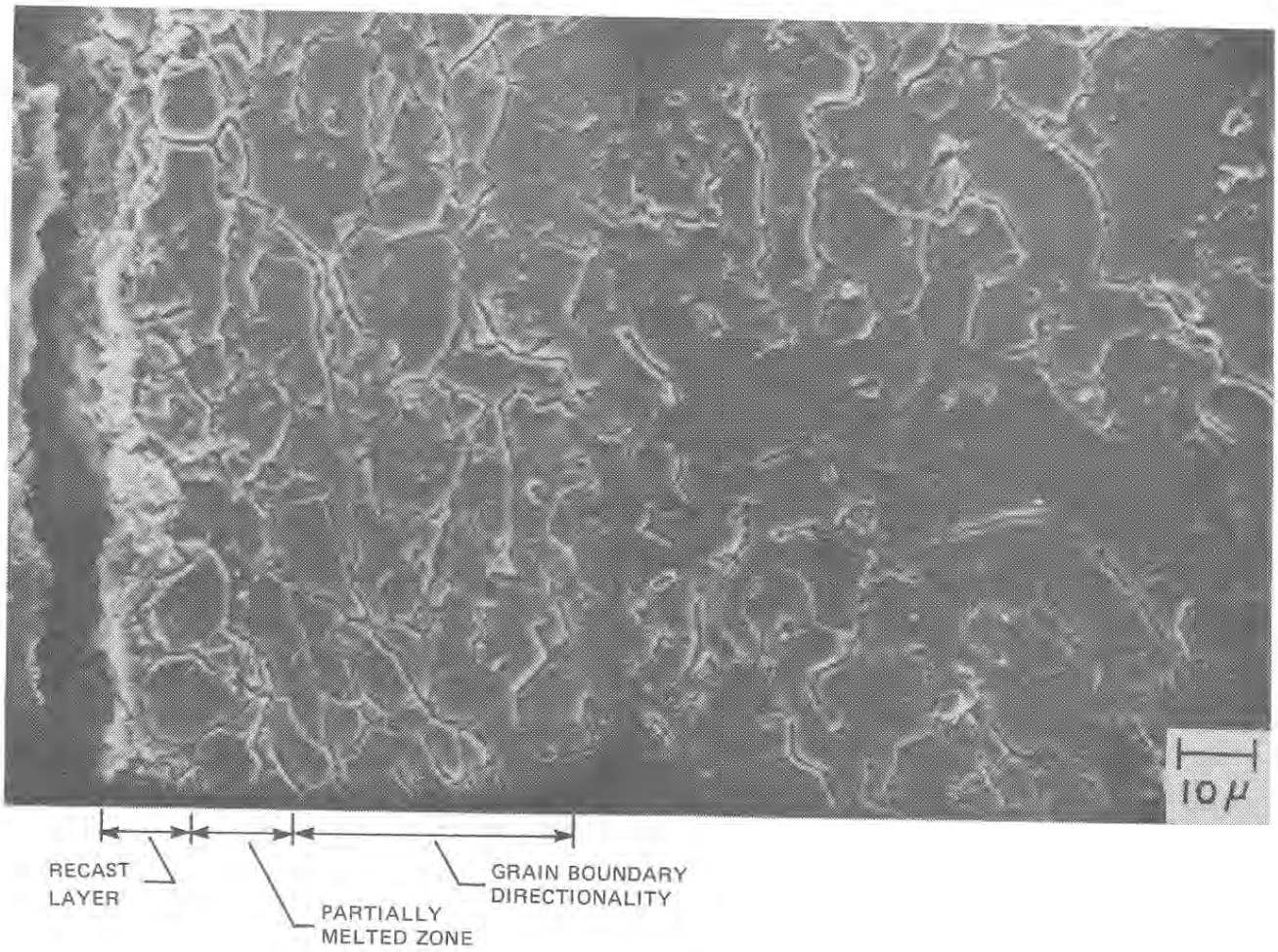

Figure 1. Cross section of a cut in sample 1 of TiB_2 showing the recast layer, partially melted zone, and a region of grain boundary directionality and grain refinement at the cut edge. Sample was polished, etched, and examined in an SEM.

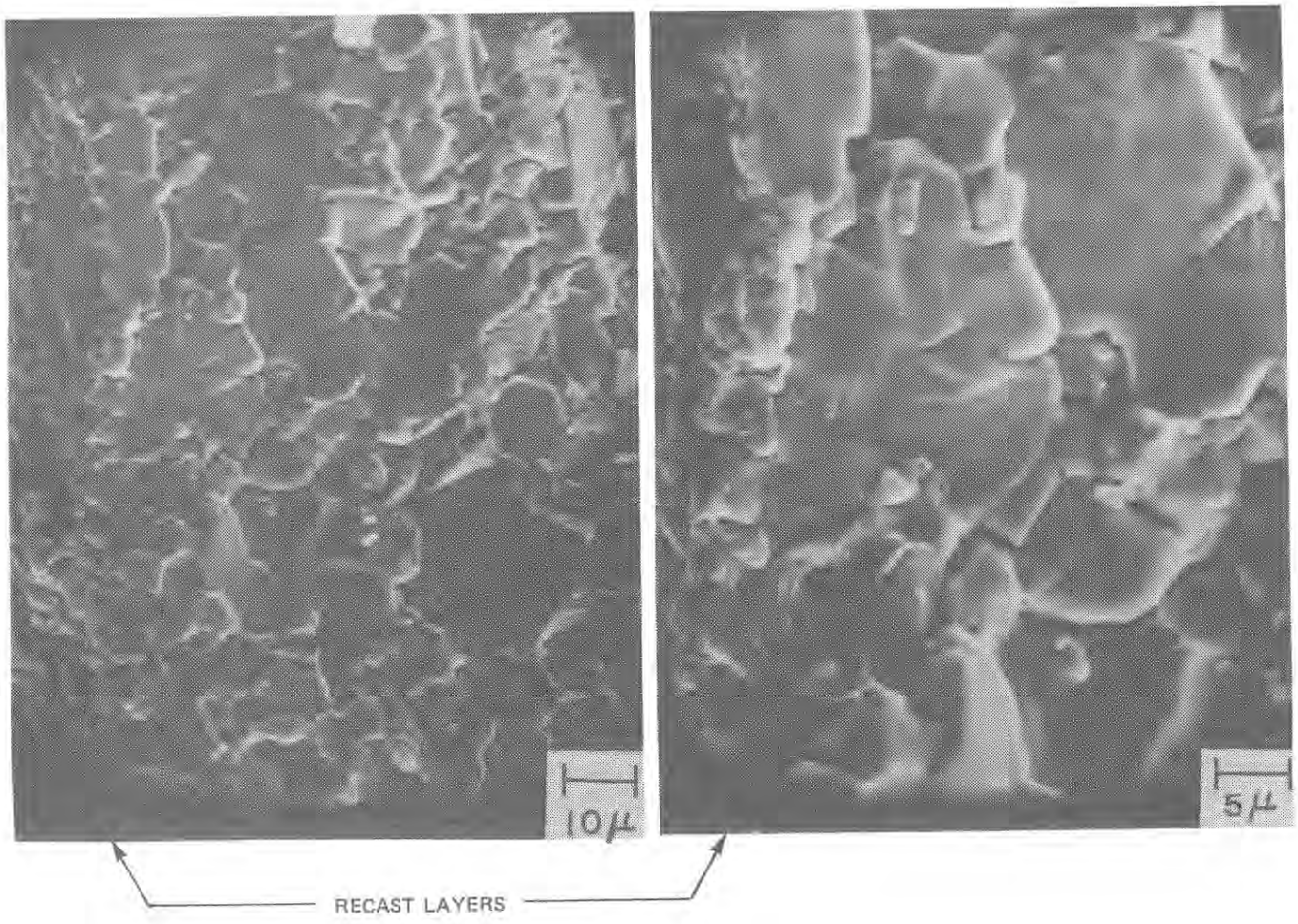

Figure 2. Fracture surface through the 30 μin. R_a EDM cut edge in sample 2d of TiB_2. Recast layer is visible on the fracture surface.

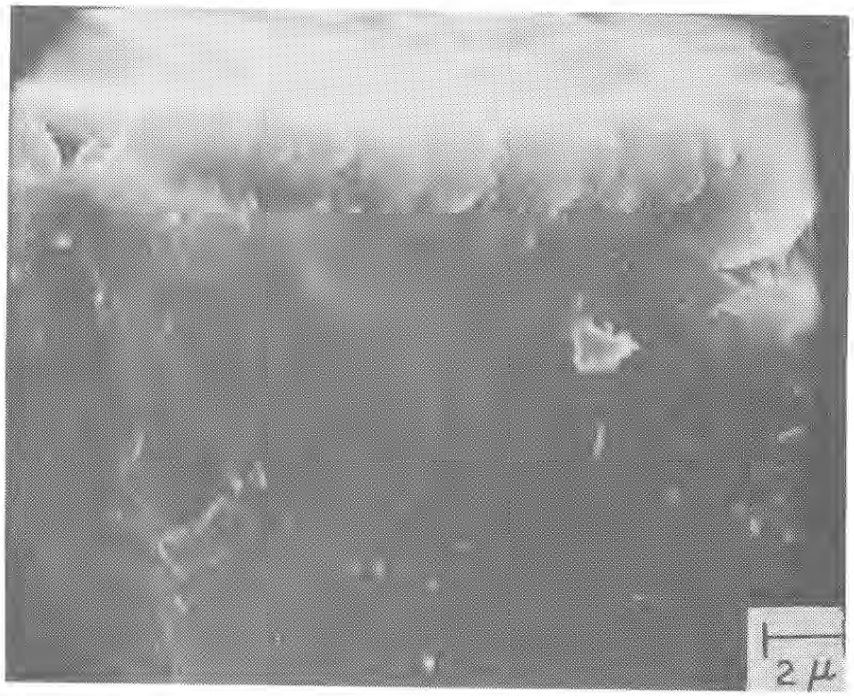

Figure 3. Fracture surface through an EDM cut edge in sample 4a showing recast layer size in a large SiC grain.

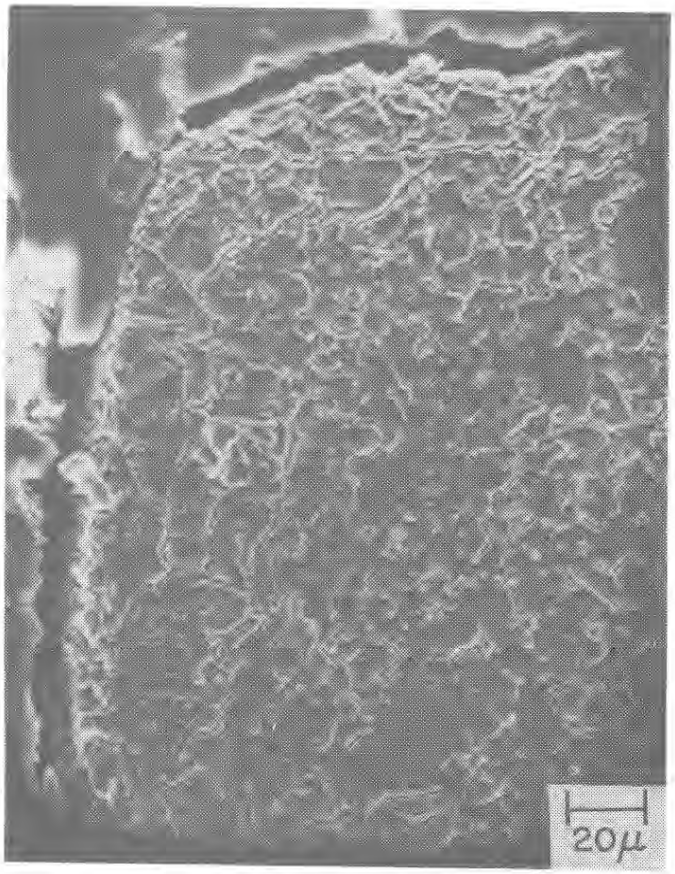

Figure 4. Cross section of a corner cut in TiB_2 showing grain boundaries near the cut edge oriented parallel to the cut surface. Sample was polished, etched, and examined in an SEM.

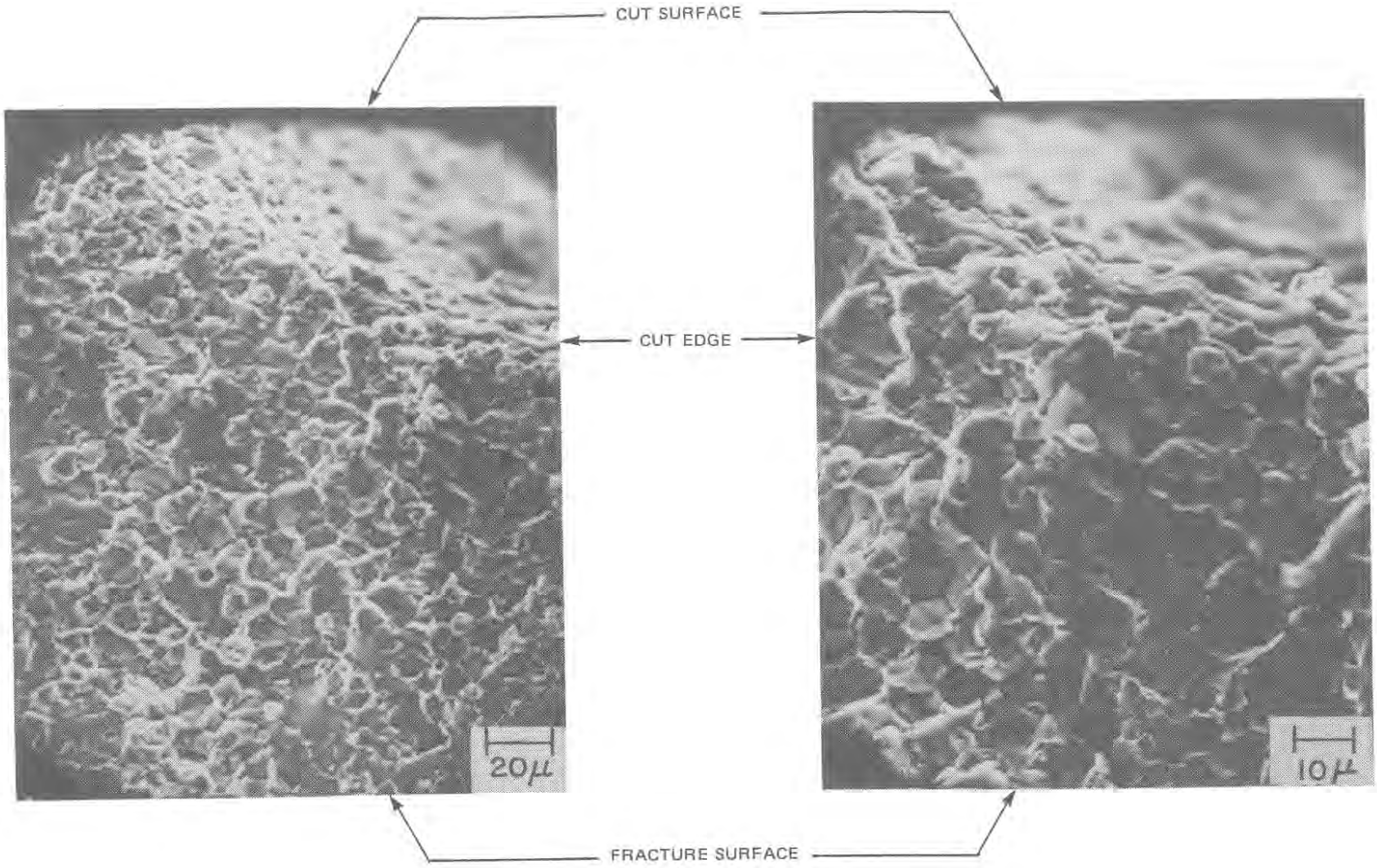

Figure 5. Fracture surface through an EDM cut edge in TiB_2 showing higher concentrations of porosity and lower levels of transgranular fracture within 50 μm of the cut surface.

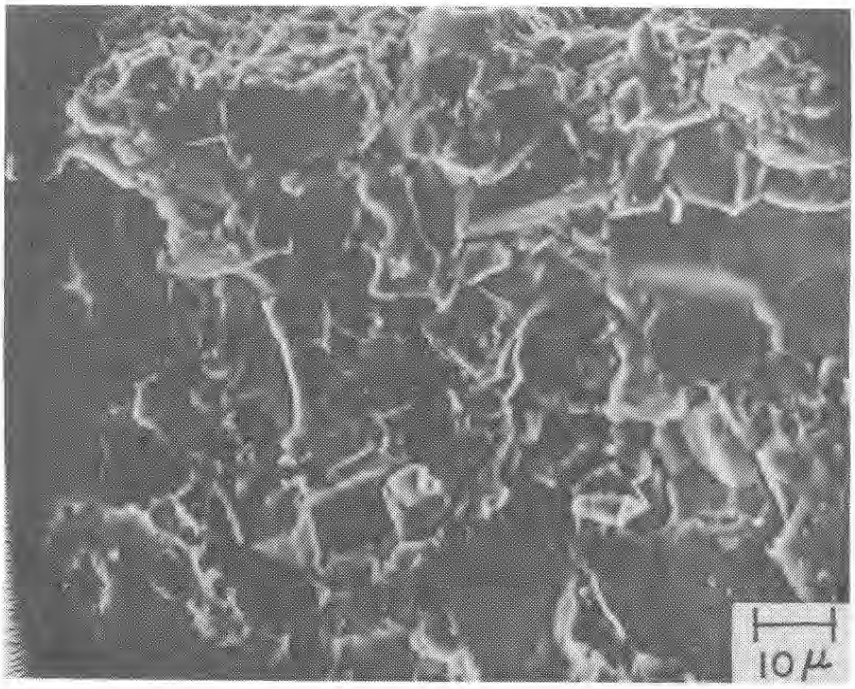

Figure 6. Fracture surface through the 70 μin. R_a cut edge of sample 2a in TiB_2 showing the roughness of the cut surface and recast layer size.

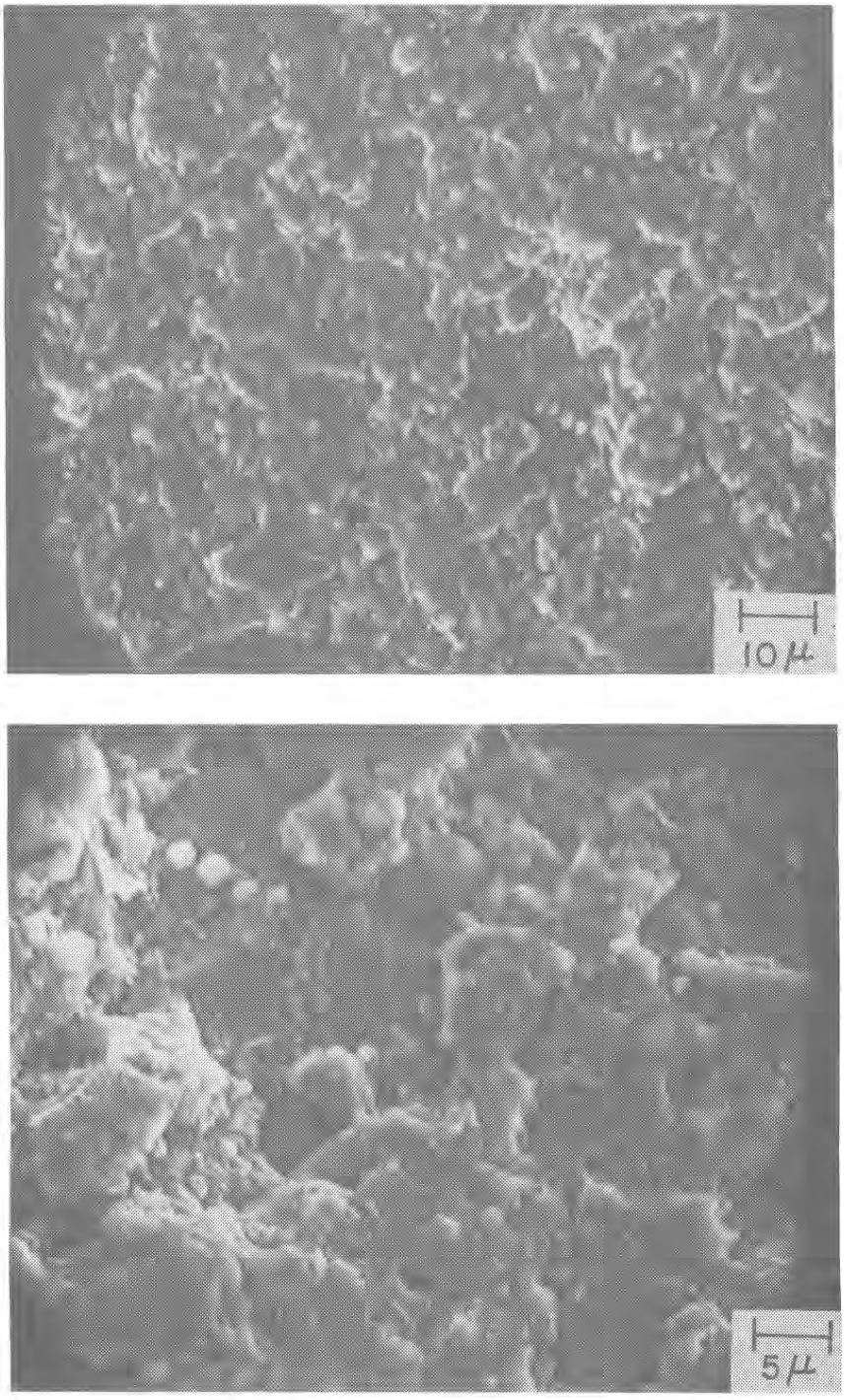

Figure 7. 30 μin. R_a cut surface in sample 2d of TiB_2.

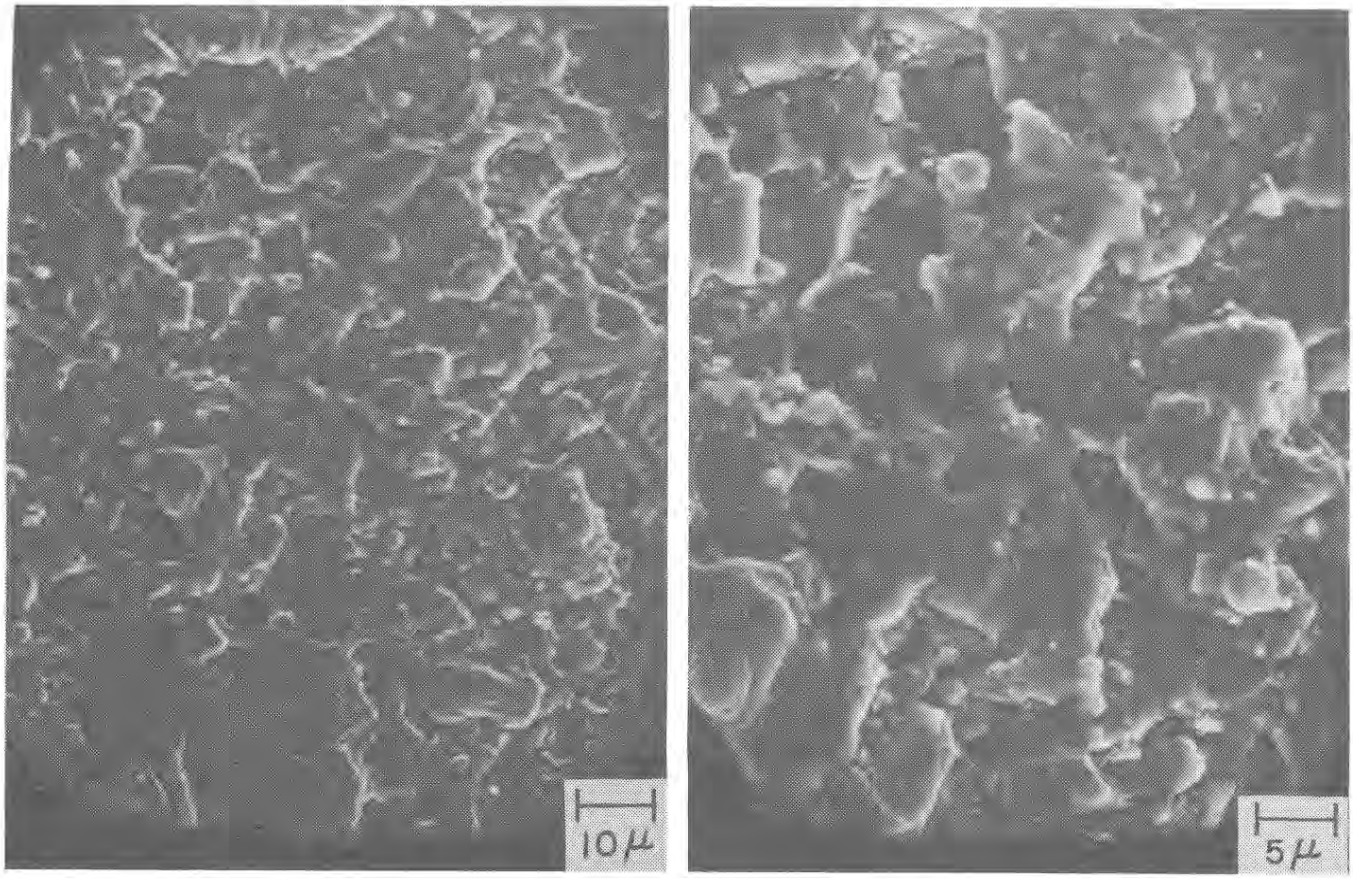

Figure 8. 55 μin. R_a cut surface in sample 2b of TiB_2.

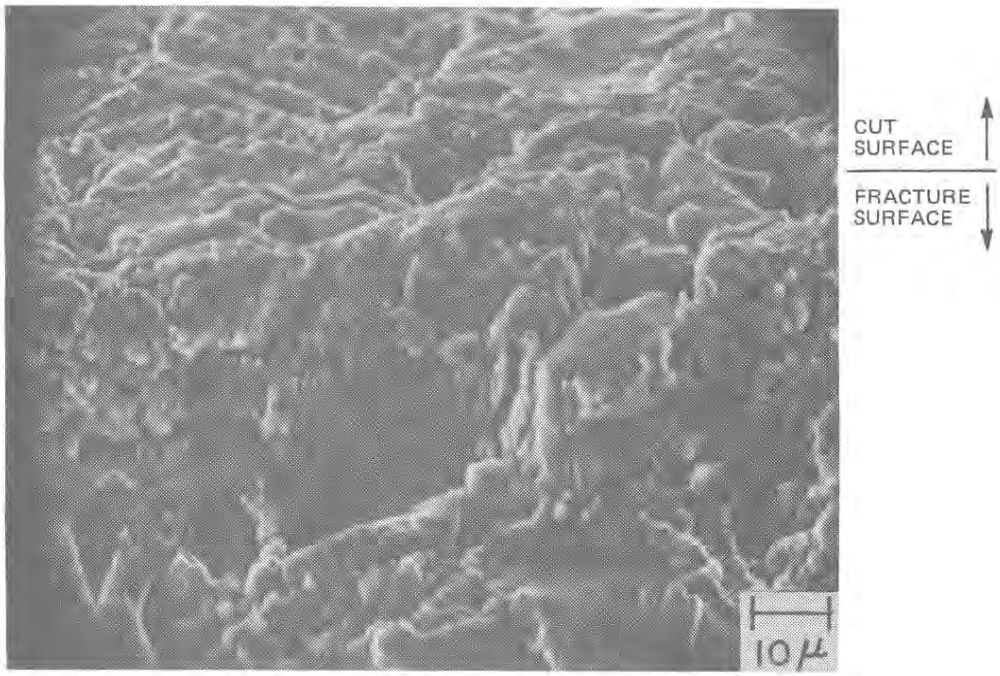

(a)

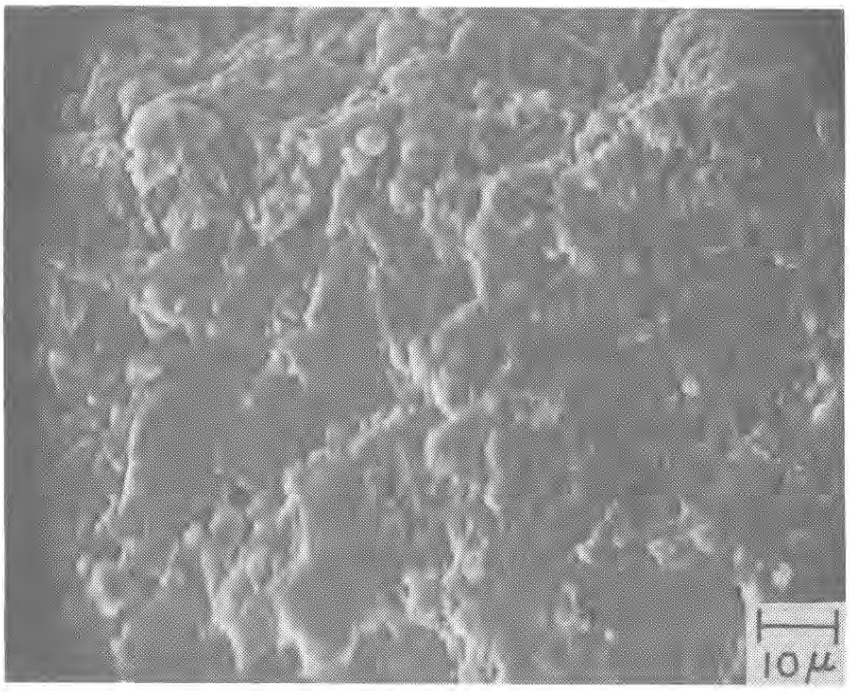

(b)

Figure 9. Fracture surface through EDM cut edges in SiC which provide low angle views of (a) the 45 μin. R_a and (b) the 70 μin. R_a cut surfaces.

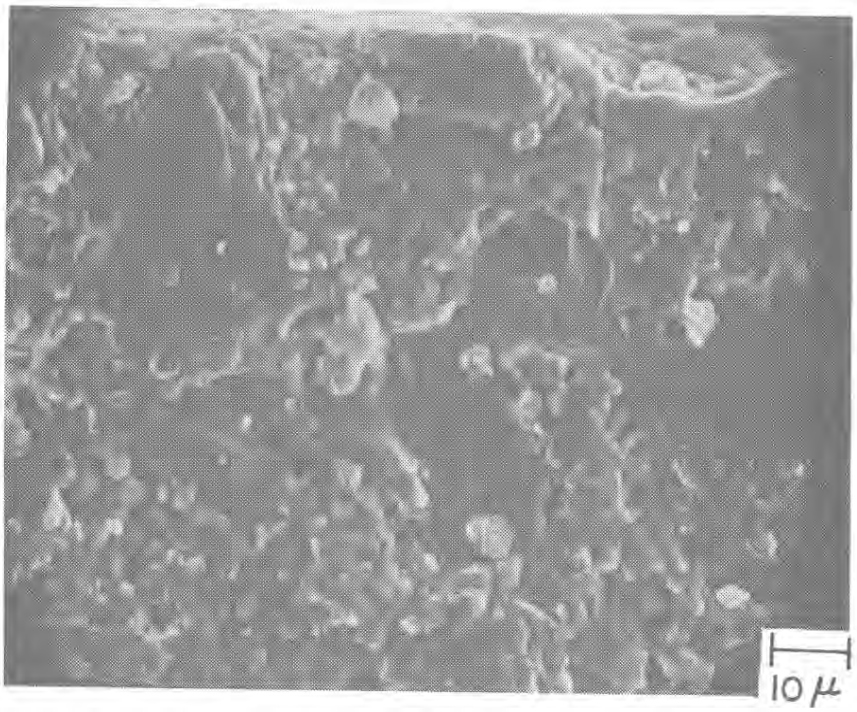

Figure 10. Fracture surface through an EDM cut edge in SiC showing preferential removal of small grains.

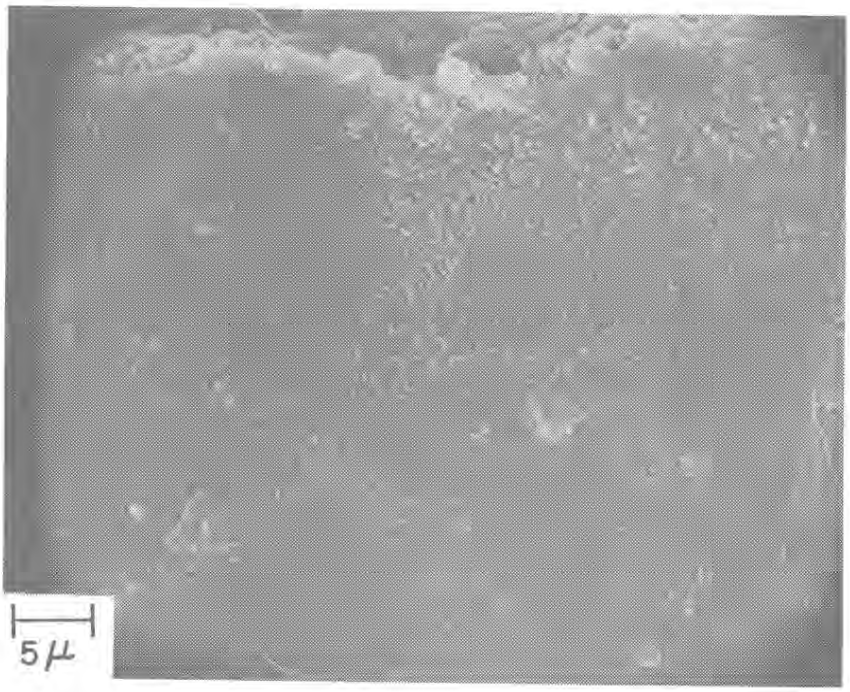

Figure 11. Fracture surface through an EDM cut edge in sample 5 of B_4C showing preferential removal of high porosity areas.

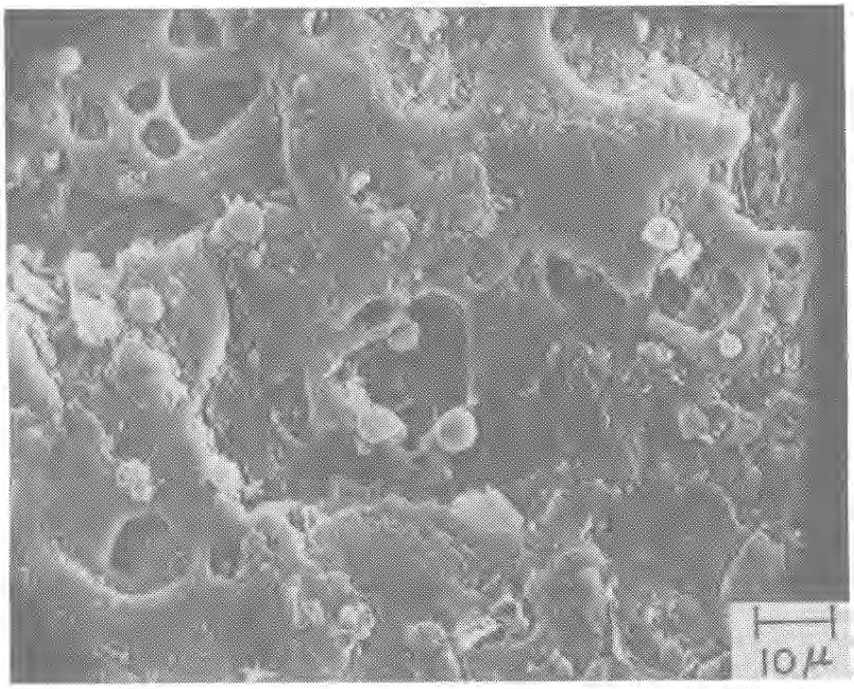

Figure 12. EDM cut surface of sample 5 in B_4C.

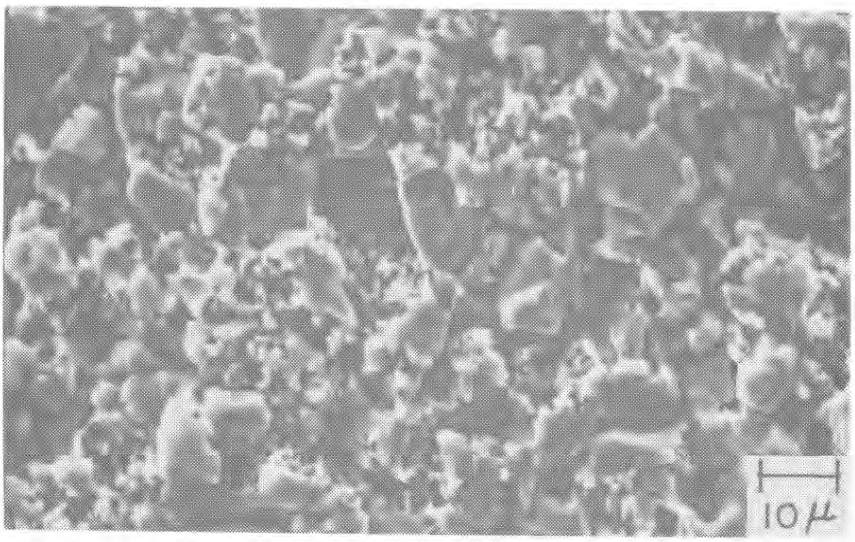

(a)

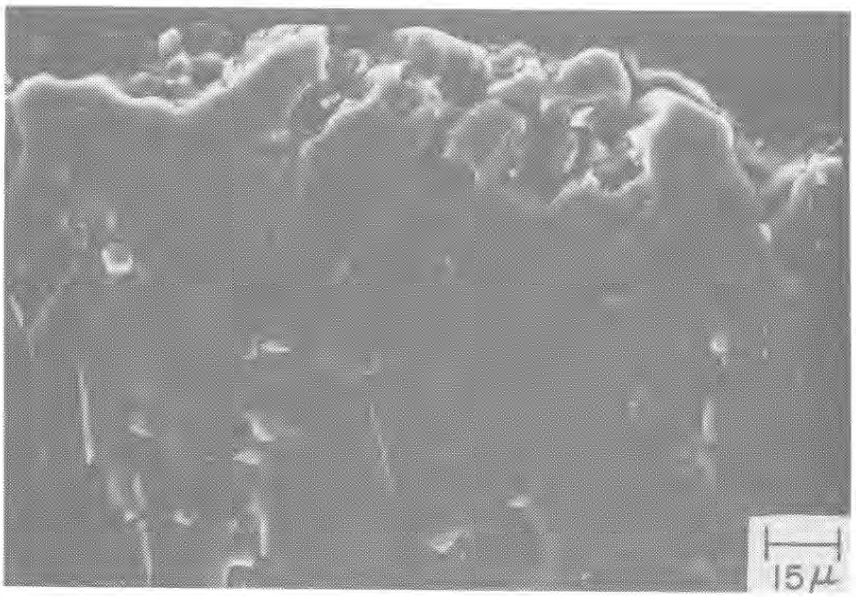

(b)

Figure 13. Extensive levels of porosity in the recast layer, (a) shown on the cut surface, and (b) polished and etched specimens through a cut.

DISTRIBUTION LIST

No. of Copies	To
1	Office of the Under Secretary of Defense for Research and Engineering, The Pentagon, Washington, DC 20301
	Commander, U.S. Army Laboratory Command, 2800 Powder Mill Road, Adelphi, MD 20783-1197
1	ATTN: Technical Library
	Commander, Defense Technical Information Center, Cameron Station, Building 5, 5010 Duke Street, Alexandria, VA 22304-6145
2	ATTN: DTIC-FDAC
	Metals and Ceramics Information Center, Battelle Columbus Laboratories, 505 King Avenue, Columbus, OH 43201
1	ATTN: Mr. Robert J. Fiorentino, Program Manager
1	Defense Advanced Research Projects Agency, Defense Sciences Office/MSD, 1400 Wilson Boulevard, Arlington, VA 22209
	Headquarters, Department of the Army, Washington, DC 20314
1	ATTN: DAEN-RDM, Mr. J. J. Healy
	Commander, U.S. Air Force Wright Aeronautical Laboratories, Wright-Patterson Air Force Base, OH 45433
1	ATTN: AFWAL/MLC
1	AFWAL/MLLP, D. M. Forney, Jr.
1	AFWAL/MLBC, Mr. Stanley Schulman
1	AFWAL/MLLS, Dr. Terence M. F. Ronald
1	AFWAL/FIBEC, Dr. Steve Johnson
1	Edward J. Morrissey, AFWAL/MLTE, Wright-Patterson Air Force Base, OH 45433
	Commander, Army Research Office, P.O. Box 12211, Research Triangle Park, NC 27709-2211
1	ATTN: Information Processing Office
1	Dr. George Mayer
	Commander, U.S. Army Materiel Command, 5001 Eisenhower Avenue, Alexandria, VA 22333
1	ATTN: AMCLD
	Commander, U.S. Army Armament, Munitions and Chemical Command, Dover, NJ 07801
1	ATTN: Mr. Harry E. Pebly, Jr., PLASTEC, Director
	Commander, U.S. Army Aviation Systems Command, 4300 Goodfellow Blvd., St. Louis, MO 63120
1	ATTN: AMDAV-NS, Harold Law
	Director, U.S. Army Ballistic Research Laboratory, Aberdeen Proving Ground, MD 21005
1	ATTN: AMDAR-TSB-S (STINFO)
	Commander, U.S. Army Electronics Research and Development Command, Fort Monmouth, NJ 07703
1	ATTN: AMDSD-L
1	AMDSD-E
	Commander, U.S. Army Foreign Science and Technology Center, 220 7th Street, N.E., Charlottesville, VA 22901
1	ATTN: Military Tech
	Commander, U.S. Army Materiel Systems Analysis Activity, Aberdeen Proving Ground, MD 21005
1	ATTN: AMXSY-MP, H. Cohen
	Commander, U.S. Army Missile Command, Redstone Scientific Information Center, Redstone Arsenal, AL 35898-5241
1	ATTN: AMSMI-RD-CS-R/ILL Open Lit
1	AMSMI-RLM
1	AMSMI-RLA, Dr. James J. Richardson

No. of Copies	To
	Commander, U.S. Army Belvoir Research, Development and Engineering Center, Fort Belvoir, VA 22060-5606
1	ATTN: STRBE-D
1	STRBE-G
1	STRBE-N
1	STRBE-VL
	Commander, U.S. Army Aviation Applied Technology Directorate, Aviation Research and Technology Activity (AVSCOM), Fort Eustis, VA 23604-5577
1	ATTN: SAVRT-TY-ATP, Mr. James Gomez, Aerospace Engineer
	Commander, U.S. Army Tank-Automotive Command, Warren, MI 48090
1	ATTN: AMSTA-RCKM
	Director, Benet Weapons Laboratory, LCWSL, USA AMCOM, Watervliet, NY 12189
1	ATTN: AMSMC-LCB-TL
1	AMSMC-LCB-PS, Dr. I. Ahmad
	David Taylor Naval Ship Research and Development Center, Annapolis, MD 21402
1	ATTN: Dr. Michael Vassilaros - Code 2814
	Office of Naval Technology, 800 N. Quincy Street, Arlington, VA 20017
1	ATTN: Mr. J. J. Kelly - Code MAT 0715
	Naval Research Laboratory, Washington, DC 20375
1	ATTN: Code 5830
1	Dr. G. R. Yoder - Code 6384
1	Dr. S. C. Sanday - Code 6370
	Chief of Naval Research, Arlington, VA 22217
1	ATTN: Code 471
1	Dr. Steven G. Fishman
	Naval Sea Systems Command, Washington, DC 20362
1	ATTN: Mr. Marlin Kinna - 62R4
	Naval Air Development Center, Warminster, PA 18974
1	ATTN: Dr. E. U. Lee - Code 60632
	Naval Surface Weapons Center, White Oak, Silver Spring, MD 20910
1	ATTN: John V. Foltz - Code R32
1	Dr. Herbert Newborn - Code R34
	National Aeronautics and Space Administration, Washington, DC 20546
1	ATTN: Mr. Michael A. Greenfield, Program Manager for Materials, Code RTM-6
	National Aeronautics and Space Administration, Lewis Research Center, Cleveland, OH 44135
1	ATTN: Dr. James A. DiCarlo, Mail Stop 106-1
	National Aeronautics and Space Administration, Marshall Space Flight Center, Huntsville, AL 35812
1	ATTN: R. J. Schwinghammer, EH01, Dir, M&P Lab
1	Mr. W. A. Wilson, EH41, Bldg. 4612
	The Boeing Vertol Company, P.O. Box 16858, Philadelphia, PA 19142
1	ATTN: Mr. Robert L. Pinckney, Mail Stop P62-06
1	Mr. Joseph P. Lenski, Jr., Mail Stop P32-09
	E. I. DuPont De Nemours and Company, Inc., Textile Fibers Department, Pioneering Research Laboratory, Experimental Station, Wilmington, DE 19898
1	ATTN: Blake R. Bichlmeir
1	Joyce W. Widrig
1	Mr. Rex C. Claridge, TRW, Incorporated, Manufacturing Division, Mail Stop 01-2210, 1 Space Park, Redondo Beach, CA 90278
1	Dr. James A. Cornie, Materials Processing Center, Bldg. 8, Room 237, Massachusetts Institute of Technology, 77 Massachusetts Avenue, Cambridge, MA 01239

No. of Copies	To
1	Dr. Bhagwan K. Das, Engineering Technology Supervisor, The Boeing Company, P.O. Box 3999, Seattle, WA 98124
1	Leroy Davis, METCO, 2225 East 28th Street, Building 5, Long Reach, CA 90806
1	Mr. Joseph F. Dolowy, Jr., President, DWA Composite Specialties, Inc., 21133 Superior Street, Chatsworth, CA 91311
1	Mr. Robert E. Fisher, President, AMERCOM, Inc., 8948 Fullbright Avenue, Chatsworth, CA 91311
1	Mr. Louis A. Gonzalez, Kaman Tempo, 816 State Street, Santa Barbara, CA 93101
1	Prof. James G. Goree, Dept. of Mechanical Engineering, Clemson University, Clemson, SC 29631
1	William F. Grant, AVCO Specialty Materials Division, 2 Industrial Avenue, Lowell, MA 01851
1	Mr. Jacob Gubbay, Charles Stark Draper Laboratories, 555 Technology Square, Mail Station 27, Cambridge, MA 02139
1	Mr. John E. Hack, Southwest Research Institute, 6220 Culebra Road, San Antonio, TX 78284
1	Dr. H. A. Katzman, The Aerospace Corporation, P.O. Box 92957 Los Angeles, CA 90009
	Lockheed California Company, Burbank, CA 91520
1	ATTN: Mr. Rod F. Simenz, Department of Materials and Processes
	Lockheed Georgia Company, 86 South Cobb Drive, Marietta, GA 30063
1	ATTN: Materials and Processes Engineering Department
1	Mr. James Carroll
	Material Concepts, Inc., 2747 Harrison Road, Columbus, OH 43204
1	ATTN: Mr. Stan J. Paprocki
1	Mr. David Goddard
1	Dr. Mohan S. Misra, Martin Marietta Aerospace, P.O. Box 179, Denver, CO 80201
1	Mr. Patrick J. Moore, Staff Engineer, Lockheed Missiles and Space Company, Organization 62-60, Building 104, P.O. Box 504, Sunnyvale, CA 94066
1	R. Byron Pipes, Professor & Director, Center for Composite Materials, University of Delaware, Newark, DE 19711
1	Dr. Karl M. Prewo, Principal Scientist, United Technologies Research Center, Mail Stop 24, East Hartford, CT 06108
1	Dr. B. W. Rosen, Materials Sciences Corporation, Gwynedd Plaza II, Bethlehem Pike, Spring House, PA 19477
1	Prof. Marc H. Richman, Division of Engineering, Brown University, Providence, RI 02912
1	Mr. Ronald P. Tye, Energy Materials Testing Laboratory, Biddeford Industrial Park, Biddeford, ME 04005
1	Mr. Robert C. Van Siclen, Vought Corporation, Advanced Technology Center, P.O. Box 226144, Dallas, TX 75266
1	Prof. Franklin E. Wawner, Department of Materials Science, School of Engineering and Applied Sciences, University of Virginia, Charlottesville, VA 22903
1	Dr. Carl Zweben, General Electric Company, Valley Forge Space Center/M4018, P.O.Box 8555, Philadelphia, PA 19101
	Director, U.S. Army Materials Technology Laboratory, Watertown, MA 02172-0001
2	ATTN: SLCMT-IML
3	Authors

☆U. S. GOVERNMENT PRINTING OFFICE: 1987--500-284--60129

U.S. Army Materials Technology Laboratory
Watertown, Massachusetts 02172-0001
WIRE-CUT ELECTRICAL DISCHARGE MACHINABILITY
OF CERAMICS - William S. Ricci,
Holly A. Skeele, and William R. Blumenthal

AD ______________

UNCLASSIFIED
UNLIMITED DISTRIBUTION

Key Words

Ceramics
Diamond grind
Electrical discharge

Technical Report MTL TR 87-52, September 1987, 23 pp -
illus-tables, D/A Project 1L263102D071,
Agency Accession DA 30 3398

The wire-cut electrical discharge machinability of four ceramics was evaluated. Titanium diboride and silicon carbide workpieces were successfully cut in the monolithic state. Boron carbide could only be cut when a metallic sandwich structure was placed around the workpiece. Silicon nitride could not be successfully cut. Mechanisms of material removal as well as a minimum level of workpiece electrical conductance necessary for EDM are proposed.

Characterization of the surface damage resulting from electrical discharge machining is presented. Recast, partially melted, and heat affected zones are identified. The effects of parametric processing variations on surface integrity are discussed. Flexure strength and residual stress data are compared for EDM cut and diamond ground surfaces in titanium diboride. Certain limitations are proposed for the EDM fabrication of ceramic components where surface defects are strength limiting.

U.S. Army Materials Technology Laboratory
Watertown, Massachusetts 02172-0001
WIRE-CUT ELECTRICAL DISCHARGE MACHINABILITY
OF CERAMICS - William S. Ricci,
Holly A. Skeele, and William R. Blumenthal

AD ______________

UNCLASSIFIED
UNLIMITED DISTRIBUTION

Key Words

Ceramics
Diamond grind
Electrical discharge

Technical Report MTL TR 87-52, September 1987, 23 pp -
illus-tables, D/A Project 1L263102D071,
Agency Accession DA 30 3398

The wire-cut electrical discharge machinability of four ceramics was evaluated. Titanium diboride and silicon carbide workpieces were successfully cut in the monolithic state. Boron carbide could only be cut when a metallic sandwich structure was placed around the workpiece. Silicon nitride could not be successfully cut. Mechanisms of material removal as well as a minimum level of workpiece electrical conductance necessary for EDM are proposed.

Characterization of the surface damage resulting from electrical discharge machining is presented. Recast, partially melted, and heat affected zones are identified. The effects of parametric processing variations on surface integrity are discussed. Flexure strength and residual stress data are compared for EDM cut and diamond ground surfaces in titanium diboride. Certain limitations are proposed for the EDM fabrication of ceramic components where surface defects are strength limiting.

U.S. Army Materials Technology Laboratory
Watertown, Massachusetts 02172-0001
WIRE-CUT ELECTRICAL DISCHARGE MACHINABILITY
OF CERAMICS - William S. Ricci,
Holly A. Skeele, and William R. Blumenthal

AD ______________

UNCLASSIFIED
UNLIMITED DISTRIBUTION

Key Words

Ceramics
Diamond grind
Electrical discharge

Technical Report MTL TR 87-52, September 1987, 23 pp -
illus-tables, D/A Project 1L263102D071,
Agency Accession DA 30 3398

The wire-cut electrical discharge machinability of four ceramics was evaluated. Titanium diboride and silicon carbide workpieces were successfully cut in the monolithic state. Boron carbide could only be cut when a metallic sandwich structure was placed around the workpiece. Silicon nitride could not be successfully cut. Mechanisms of material removal as well as a minimum level of workpiece electrical conductance necessary for EDM are proposed.

Characterization of the surface damage resulting from electrical discharge machining is presented. Recast, partially melted, and heat affected zones are identified. The effects of parametric processing variations on surface integrity are discussed. Flexure strength and residual stress data are compared for EDM cut and diamond ground surfaces in titanium diboride. Certain limitations are proposed for the EDM fabrication of ceramic components where surface defects are strength limiting.

U.S. Army Materials Technology Laboratory
Watertown, Massachusetts 02172-0001
WIRE-CUT ELECTRICAL DISCHARGE MACHINABILITY
OF CERAMICS - William S. Ricci,
Holly A. Skeele, and William R. Blumenthal

AD ______________

UNCLASSIFIED
UNLIMITED DISTRIBUTION

Key Words

Ceramics
Diamond grind
Electrical discharge

Technical Report MTL TR 87-52, September 1987, 23 pp -
illus-tables, D/A Project 1L263102D071,
Agency Accession DA 30 3398

The wire-cut electrical discharge machinability of four ceramics was evaluated. Titanium diboride and silicon carbide workpieces were successfully cut in the monolithic state. Boron carbide could only be cut when a metallic sandwich structure was placed around the workpiece. Silicon nitride could not be successfully cut. Mechanisms of material removal as well as a minimum level of workpiece electrical conductance necessary for EDM are proposed.

Characterization of the surface damage resulting from electrical discharge machining is presented. Recast, partially melted, and heat affected zones are identified. The effects of parametric processing variations on surface integrity are discussed. Flexure strength and residual stress data are compared for EDM cut and diamond ground surfaces in titanium diboride. Certain limitations are proposed for the EDM fabrication of ceramic components where surface defects are strength limiting.